Preprints of the 19th World Congress
The International Federation of Automatic Control
Cape Town, South Africa. August 24-29, 2014

A distributed braking control algorithm with preview action for railroad vehicles ⋆

Bruno Picasso * **Danilo Caporale** * **Patrizio Colaneri** *

* *DEIB, Politecnico di Milano, Piazza Leonardo da Vinci 32, 20133 Milano, Italy*
(e-mail: picasso-caporale-colaneri@elet.polimi.it*)*

Abstract: A method is proposed to enhance the overall braking performance of a railroad vehicle (train) by properly exchanging information among the single control units. Taking advantage of data transmitted from the coaches at the front of the train to the rear carriages, a novel distributed braking control algorithm is proposed that, based on preview control techniques, allows one to reduce the stopping distance. The algorithm is demonstrated and compared to other standard approaches through simulations.

Keywords: Braking control systems; preview control; optimal control.

1. INTRODUCTION

Active braking forces in train dynamics are generated at the contact points between the wheels and the rails. Translating and rotating masses dynamics can be modeled through linear systems, while the contact force is a nonlinear function of the states [Olson et al. 2003, Polach 2005]. This function, referred to as the adherence curve, describes the relation between the slip (*i.e.,* the relative difference between the speed of the wheels and of the translating mass) and the friction coefficient. This curve exhibits one global optimum point, which is the desired working condition as it allows the maximum adherence of the vehicle to the rail and, in a braking maneuver, the maximum deceleration of the vehicle. When, instead, the current slip value crosses over this maximum, the wheels tend to lock and the braking force reduces, thus resulting in a bad braking performance and a damage of both the wheels and the rails. An accurate description of this phenomena can be found in [Olson et al. 2003].

Anti–slip braking control systems (ABCS) are typically used to prevent the wheels from locking and, as a result, to reduce the braking distance. With this goal in mind, the system is typically controlled to achieve stability in the neighborhood of a reference slip value. The major drawback of this approach is the dependence of the braking distance on the knowledge of a correct reference value. On the other side, more aggressive approaches can be used, where the stabilization and the optimal working point estimation are simultaneously performed. For instance, in [Ariyur and Krstić 2003] this goal is achieved with extremum seeking techniques. In a recent work [Caporale et al. 2013], a nonlinear adaptive control strategy was used to perform this task without the injection of external harmonic signals. Another example of ABCS based on adaptive control can be found in [Tyukin 2011].

The adherence curve mainly depends on three factors [Polach 2005]: at a low level, the friction is affected by the physical and geometrical characteristics of the contacting surfaces between the wheel and the rail (however, such a level of detail can be disregarded in ABCS design). At higher levels, the presence of contaminants on the rail and the speed of the train are important elements, which can be captured with model based approaches (a function whose parameters are estimated online) or extremum seeking methods with the above described techniques.
Focus in the literature has been mainly given to the behavior of a single ABCS. As a result, an important element in railway ABCS has not received sufficient attention: the rail itself. Trains are constrained to advance on a railroad. As such, wheels in the back coaches are constantly heading for conditions that the preceding coaches have already met moments before. Related to this issue, a well–known effect in the railway industry is the rail cleaning. This happens when, for example, water is on the rail which is partially removed as a wheel passes over it. As a consequence, the available braking force is increasing as more and more wheels pass over a certain point of the rail. This phenomenon has been treated in [Imai et al. 2010], where the problem of balancing the braking–force along the train between all the controllers has been studied.
In this framework, the present paper proposes an investigation on the possibility of taking advantage of information exchanges between preceding and following coaches in order to improve the braking performance and to reduce the stopping distance of the train. Different braking control approaches are considered depending on the level of communication between the control units. In particular, a novel distributed braking control algorithm is proposed that, thank to the preview of the future condition of the rail offered by the coaches at the front of the train, is capable of better tracking the maximum adherence condition. In so doing, it is possible to enhance the performance offered by the single control units and to reduce the stopping distance as compared to standard techniques based on limited (or lacking in) communication.

⋆ This work was performed in part whilst Danilo Caporale was a visiting student at the M.I.T. Corresponding author: Bruno Picasso.

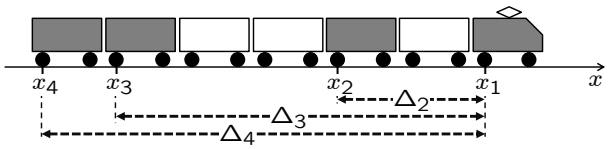

Figure 1. Example of train configuration: the grey coaches are those with braking capability.

The proposed control strategy is grounded on the theory of preview control (see, *e.g.,* [Middleton et al. 2004, Moelja and Meinsma 2006]) but, due to the nonlinearity of the model, we could not prove optimality. Extensive simulations have been hence performed to test and compare our algorithm with standard techniques. The numerical experiments confirmed the soundness of the preview control based strategy and regularly showed that it outperforms the other techniques. Special attention is devoted to understanding the part played by the various parameters in the problem, such as the distance between the actuated coaches and the convergence rate of the control units.
In this work, the focus has been placed on the role of communication and preview for performance improvements. As such, the dependence of the adherence curve on the train state is expressed only by its dependence on the position and on the traveling speed. Other effects, such as the above mentioned cleaning effect, have not been considered here and they are the subject of current work.

Paper organization: in Section 2, a model for the considered system is presented where the wheel–rail contact description is based on [Olson et al. 2003, Caporale et al. 2013]; hence, the different braking control algorithms and, in particular, the novel distributed preview control strategy are defined. Detailed simulation comparisons between the three considered approaches are reported in Section 3. Conclusions and future research are outlined in Section 4.

2. BRAKING CONTROL ALGORITHMS

2.1 The models

Consider a railroad vehicle (train) where n coaches are equipped with a braking control system and let $x_1 > x_2 > \cdots > x_n$ be the positions of such devices. The train is considered as a rigid body running at a speed $v(t)$, thus the distance $\Delta_i = x_1 - x_i$ is constant, see Figure 1.

Model of the adherence coefficient. The adherence coefficient between the wheel and the rail is denoted by μ. Its dependence on the physical characteristics of the rail at x, on the wheel angular speed ω and on the speed v of the train is modeled as follows: let the (relative) slip be

$$\sigma(\omega, v) = \tfrac{v - R\omega}{v},$$

where R is the wheel radius and $\sigma \in [\,0\,,\,1\,]$ because we are considering a braking maneuver; the adherence curve is

$$\bar{\mu}\big(\theta(x), \sigma\big) = \tfrac{\sqrt{\sigma}}{\theta_1(x) + \theta_2(x)\sigma + \theta_3(x)\sigma^2};$$

finally, we consider

$$\mu\big(\theta(x), \sigma, v\big) = \frac{1}{k_1(v)} \cdot \bar{\mu}\big(\theta(x), k_2(v)\sigma\big), \tag{1}$$

where $k_i(v) = 1 + \pi_i v$, for suitable constants $\pi_i > 0$.
In so doing, $\bar{\mu}\big(\theta(x), \sigma\big) = \mu\big(\theta(x), \sigma, 0\big)$: the physical characteristics of the rail are described through the parameters $\theta(x) \in \mathbb{R}^3$ and summed up in the function $\bar{\mu}\big(\theta(x), \sigma\big)$ whereas, under the same characteristics, the coefficients $k_i(v)$ are used to parameterize the dependence of μ on the speed. Therefore, a rail with spatially varying adherence characteristics is represented by a non-constant function $\theta(x)$. Consider the maximizer $\bar{\sigma}^o(x)$ of $\bar{\mu}$ at x, *i.e.,*

$$\bar{\sigma}^o(x) = \tfrac{-\theta_2(x) + \sqrt{\theta_2^2(x) + 12\theta_1(x)\theta_3(x)}}{6\theta_3(x)},$$

and let $\bar{\mu}^o(x) = \bar{\mu}\big(\theta(x), \bar{\sigma}^o(x)\big)$ be the corresponding maximal value. The following relations hold for the maximizer $\sigma^o(x, v)$ of μ and the maximal value $\mu^o(x, v)$:

$$\begin{cases} \sigma^o(x, v) = \frac{\bar{\sigma}^o(x)}{k_2(v)} \\ \mu^o(x, v) = \frac{1}{k_1(v)} \bar{\mu}^o(x). \end{cases} \tag{2}$$

This is consistent with the well–known fact that the increase of v causes both the decrease of the maximum achievable adherence μ^o and of the maximizing slip σ^o (see the literature on creep forces, such as [Polach 2005]).

Model of the speed dynamics. If the effects of the total mass of the train are equally shared among the n actuated coaches, the model for the speed dynamics is

$$\dot{v}(t) = -g \frac{\sum_{i=1}^{n} \mu\big(\theta(x_1(t) - \Delta_i), \sigma_i(t), v(t)\big)}{n}, \tag{3}$$

where $\sigma_i(t)$ is the slip of the i–th wheel at time t.

Model of the slip dynamics. The model of the closed–loop (relative) slip dynamics, embedded within each braking control unit, is approximated by the following unitary gain first order linear system:

$$\dot{\sigma}_i(t) = -\alpha\sigma_i(t) + \alpha\Sigma_i^o(t),\ i = 1, \ldots, n, \tag{4}$$

where $\Sigma_i^o(t)$ is the reference signal for the i–th controller and $\alpha > 0$ is the inverse of the time constant characterizing such closed–loop dynamics. In other words, the antiskid control devices are supposed to be capable of precisely tracking their reference. For a control algorithm with adherence estimation and capable of tracking the maximum adherence slip condition σ^o, see *e.g.,* [Caporale et al. 2013].

2.2 The reference generation: three different approaches

In view of equation (3), in order to reduce the stopping distance, the control objective is to maintain the slip σ_i as close as possible to the optimal value $\sigma^o(x_i, v)$ maximizing the adherence μ between the wheel of the i–th coach and the rail. To this end, different algorithms for the generation of the reference signal $\Sigma_i^o(t)$ in equation (4) are considered:

(1) *Leader–follower approach* (Lf). The coaches share a common reference signal corresponding to the optimal slip value for the first coach:
$$\Sigma_i^o(t) = \sigma^o\big(x_1(t), v(t)\big),\ i = 1, \ldots, n.$$
(2) *Blind decentralized approach* (Bd). Each coach tracks its own optimal slip value:
$$\Sigma_i^o(t) = \sigma^o\big(x_i(t), v(t)\big),\ i = 1, \ldots, n.$$

The main interest for the Lf algorithm lies in its simplicity of implementation. The Bd approach, instead, is typically adopted in practical applications as it does not require information exchange between the control units. However, braking performance can be enhanced if communication between the controllers is allowed. According to the pre-

view control philosophy [Middleton et al. 2004, Moelja and Meinsma 2006], the optimal slip value $\sigma^o\big(x_i(t), v(t)\big)$ can be better tracked if a preview on its future behavior is available. This is possible, indeed, because the i–th controller can take advantage of the information on σ^o already acquired by the $i-1$ coaches placed in front of him. Hence, an innovative third algorithm is considered:

(3) *Distributed preview approach* (Dp). Each coach tracks its optimal slip value anticipated of a suitable and possibly non-constant time interval $\tau_i(t)$:

$$\Sigma_i^o(t) = \sigma^o\Big(x_i\big(t+\tau_i(t)\big), v\big(t+\tau_i(t)\big)\Big),\ i=1,\dots,n.$$

2.3 The design of the distributed preview algorithm

The optimal slip value σ^o is intrinsically related to the physical characteristics of the rail, as such, it is useful to express it as a function of the position of the train on the rail. Let us hence rewrite model (4) by replacing the time variable t with the position x_1 of the first coach. To this end, consider a function $z\big(x_1(t)\big)$: since

$$\tfrac{dz}{dt} = \tfrac{dz}{dx_1}\cdot\tfrac{dx_1}{dt} = \tfrac{dz}{dx_1}\cdot v(t),$$

then, as long as $v(t) > 0$, the differential equations in x_1 are simply obtained by dividing the equations in the variable t by v. Thus, denoting by z' the derivative of z with respect to x_1, $\forall\, i=1,\dots,n$, one has

$$\sigma_i'(x_1) = -\frac{\alpha}{v(x_1)}\sigma_i(x_1) + \frac{\alpha}{v(x_1)}\Sigma_i^o(x_1). \tag{5}$$

Remark 1. Notice that $\sigma_i(x_1)$ represents the slip of the wheel in the i–th coach when the first coach (not the i–th one) is located at x_1. In other words, the clock governing equation (5) is driven by the moving on of the first coach.

The first coach has not preview capability, hence we let

$$\Sigma_1^o(x_1) = \sigma^o\big(x_1, v(x_1)\big).$$

Let us consider the i–th coach for $i>1$: assume for the moment that the speed $v(x_1)$ is constant and let $\lambda = \frac{\alpha}{v(x_1)}$, then equation (5) rewrites as

$$\sigma_i'(x_1) = -\lambda\sigma_i(x_1) + \lambda\Sigma_i^o(x_1). \tag{6}$$

Letting $r^o(x_1) = \sigma^o\big(x_1, v(x_1)\big)$, the optimal slip value at the location of the i–th coach is given by $r^o(x_1-\Delta_i)$. Therefore, in accordance with Remark 1, the goal is to make $\sigma_i(x_1)$ track $r^o(x_1-\Delta_i)$. To this end, the forward behavior $r^o(x_1-\delta_i)$, $0\le\delta_i\le\Delta_i$, is available to the i–th braking control unit and this information can be profitably used to improve the tracking performance. For instance, consider a step variation[1] $r^o(x_1) = H(x_1)$ of the optimal slip and let us look for the value of δ_i so that, letting $\Sigma_i^o(x_1) = r^o(x_1-\delta_i)$ $\big($and $\sigma_i(0)=0\big)$ in equation (6), the $\mathcal{L}^2$–norm of the tracking error

$$e_i(x_1) = r^o(x_1-\Delta_i) - \sigma_i(x_1)$$

is minimized. Easy computations show that

$$e_i(x_1) = H(x_1-\Delta_i) - H(x_1-\delta_i)\big(1-e^{-\lambda(x_1-\delta_i)}\big) \tag{7}$$

and

$$\|e_i\|_2^2 = \int_0^{+\infty} e_i^2(x_1)dx_1 = \Delta_i - \delta_i + \tfrac{1}{\lambda}\left(2e^{-\lambda(\Delta_i-\delta_i)} - \tfrac{3}{2}\right),$$

[1] Where, as usual, $H(x_1) = \begin{cases} 0 \text{ if } x_1<0 \\ 1 \text{ if } x_1\ge 0. \end{cases}$

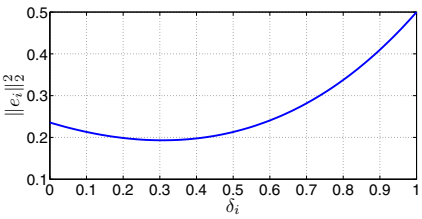

Figure 2. Behavior of $\|e_i\|_2^2$ for $\lambda=1$ and $\Delta=1$.

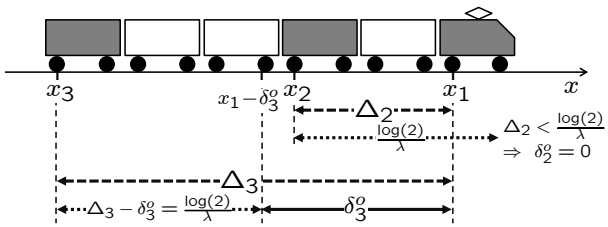

Figure 3. Example of locations of the points whose corresponding optimal value σ^o is tracked by the i–th coach: since $\Delta_2 < \frac{\log(2)}{\lambda}$, then $\delta_2^o = 0$ and $\Sigma_2^o(x_1) = \sigma^o\big(x_1, v(x_1)\big)$; $\Sigma_3^o(x_1) = \sigma^o\big(x_1-\delta_3^o, v(x_1)\big)$.

so that

$$\operatorname{argmin}_{\delta_i}\|e_i\|_2^2 = \Delta_i - \tfrac{\log(2)}{\lambda}$$

and, since $\delta_i\ge 0$, the optimal value δ_i^o is given by

$$\delta_i^o = \max\left\{0\,,\ \Delta_i - \tfrac{\log(2)}{\lambda}\right\}$$

(see also Figure 2). This means that, in the presence of a step variation $r^o(x_1) = H(x_1)$, the $\mathcal{L}^2$–norm minimization of the tracking error is obtained by feeding system (6) with

$$\Sigma_i^o(x_1) = \sigma^o\big(x_1-\delta_i^o, v(x_1)\big), \tag{8}$$

that is a reference corresponding to the optimal slip value σ^o at a point which is placed in front of the i–th coach at a distance $\Delta_i-\delta_i^o$ (see Figure 3).

The optimality of δ_i^o is not limited to step variations of $r^o(x_1)$. In fact, denote by

$$T_{\delta_i}(s) = e^{-\Delta_i s} - \tfrac{\lambda}{s+\lambda}e^{-\delta_i s}$$

the transfer function from $r^o(x_1)$ to $e_i(x_1)$ and let

$$W_{\delta_i}(s) = \tfrac{1}{s}\cdot T_{\delta_i}(s),$$

then $e_i(x_1)$ in equation (7) is the impulse response of system $W_{\delta_i}(s)$ so that δ_i^o minimizes the $\mathcal{H}^2$–norm of $W_{\delta_i}(s)$. Recalling that the $\mathcal{H}^2$–norm is equal to the $\mathcal{L}^\infty/\mathcal{L}^2$–gain, then δ_i^o also guarantees the minimization of the worst–case $\mathcal{L}^\infty$–norm of the error e_i at the varying of all input signals $r^o(x_1)$ whose derivative belongs to $\mathcal{L}^2$ and has an $\mathcal{L}^2$–norm below any fixed value $\gamma>0$. Moreover, numerical experiments show that δ_i^o also minimizes the $\mathcal{H}^\infty$–norm of $W_{\delta_i}(s)$: since the $\mathcal{H}^\infty$–norm is equal to the $\mathcal{L}^2/\mathcal{L}^2$–gain, then for the same class of input signals specified above, also the worst case $\mathcal{L}^2$–norm of the error e_i is minimized.

Let us now consider the realistic case where $v(x_1)$ is not constant. The optimization of δ_i is now impractical because, due to the nonlinear dynamics of $v(x_1)$, the dynamics of σ_i is varying with x_1 in a nonlinear fashion. Nonetheless, the achieved result is expected to be close to the optimum as long as the dynamics of σ_i is faster than the dynamics of v. Recalling that $\lambda = \frac{\alpha}{v(x_1)}$, we hence replace the constant δ_i^o with the following speed dependent

expression:

$$\delta_i^*\big(v(x_1)\big) = \max\left\{0\,,\,\Delta_i - \frac{v(x_1)\log(2)}{\alpha}\right\}. \qquad (9)$$

Then, consistently with the expression in equation (8), let

$$\Sigma_i^o(x_1) = \sigma^o\big(x_1 - \delta_i^*, v(x_1 + \Delta_i - \delta_i^*)\big),$$

where $v(x_1 + \Delta_i - \delta_i^*)$ is the speed of the train when the i–th coach will reach the point $x_1 - \delta_i^*$ (the dependence of δ_i^* on $v(x_1)$ has been omitted for the sake of clarity in the notation). Nevertheless, since $v(x_1 + \Delta_i - \delta_i^*)$ is not available, then a prediction based on the following first–order hold model is considered:

$$\hat{v}(x_1 + \Delta_i - \delta_i^*) = v(x_1) + v'(x_1)(\Delta_i - \delta_i^*). \qquad (10)$$

Accordingly, for $i > 1$, the reference signal for system (5) is given by

$$\Sigma_i^o(x_1) = \sigma^o\big(x_1 - \delta_i^*, \hat{v}(x_1 + \Delta_i - \delta_i^*)\big).$$

Finally, for $n = 2$ coaches with breaking capability, the overall system under the Dp algorithm is given by

$$\begin{cases} \sigma_1'(x_1) = -\frac{\alpha}{v(x_1)}\sigma_1(x_1) + \frac{\alpha}{v(x_1)}\sigma^o\big(x_1, v(x_1)\big) \\ \sigma_2'(x_1) = -\frac{\alpha}{v(x_1)}\sigma_2(x_1) + \frac{\alpha}{v(x_1)}\sigma^o\big(x_1 - \delta_2^*, \hat{v}(x_1 + \Delta_2 - \delta_2^*)\big) \\ v'(x_1) = -\frac{g}{2v(x_1)}\big[\mu\big(\theta(x_1), \sigma_1(x_1), v(x_1)\big) + \\ \qquad\qquad + \mu\big(\theta(x_1 - \Delta_2), \sigma_2(x_1), v(x_1)\big)\big], \end{cases} \qquad (11)$$

where $\sigma^o(x, v)$ and $\mu(\theta, \sigma, v)$ are given in equations (2) and (1), respectively, $\hat{v}(x_1 + \Delta_2 - \delta_2^*)$ is in equation (10) and the equation for $v'(x_1)$ has been derived by equation (3). The extension of model (11) to $n \geq 3$ is straightforward.

Remark 2. For implementation purposes, it may be useful to rewrite model (11) in the standard form of a system of differential equations in the time variable t, that is:

$$\begin{cases} \dot{x}_1(t) = v(t) \\ \dot{\sigma}_1(t) = -\alpha\sigma_1(t) + \alpha\sigma^o\big(x_1(t), v(t)\big) \\ \dot{\sigma}_2(t) = -\alpha\sigma_2(t) + \alpha\sigma^o\Big(x_1\big(t - \tau_2^*(t)\big), \hat{v}\big(t + T_2^*(t)\big)\Big) \\ \dot{v}(t) = -\frac{g}{2}\big[\mu\big(\theta(x_1(t)), \sigma_1(t), v(t)\big) + \\ \qquad\qquad + \mu\big(\theta(x_1(t) - \Delta_2), \sigma_2(t), v(t)\big)\big], \end{cases}$$

where $t - \tau_2^*(t)$ is the instant when the first coach was located at $x_1(t) - \delta_2^*\big(v(t)\big)$, thus $\tau_2^*(t)$ is such that

$$\int_{t-\tau_2^*(t)}^{t} v(\zeta)d\zeta = \delta_2^*\big(v(t)\big),$$

$\hat{v}(t + T_2) = v(t) + \dot{v}(t)T_2$ and $t + T_2^*(t)$ is the instant when the second coach is expected to reach the point $x_1(t) - \delta_2^*\big(v(t)\big)$ (*i.e.,* the first coach has reached the point $x_1(t) + \Delta_2 - \delta_2^*\big(v(t)\big)\big)$, thus $T_2^*(t)$ is such that

$$\int_0^{T_2^*(t)} \hat{v}(t + \zeta)d\zeta = \Delta_2 - \delta_2^*\big(v(t)\big).$$

3. SIMULATIONS COMPARISON

In the following section the performance of the three proposed algorithms are compared through simulations. We have generated a function $\theta(x)$ to model a rail of 1000 m in length, characterized by different physical conditions (ranging from extra dry to extra wet) that pass by one after the other both in a discontinuous fashion and in a more smooth manner. The corresponding behaviors of $\bar{\mu}^o(x)$ and of $\bar{\sigma}^o(x)$ are reported in Figure 4 (other profiles have been considered as well and the obtained results were coherent with those presented here). As for $k_1(v)$ and $k_2(v)$, we made the conventional (yet realistic) assumption that

$$k_1(v) = k_2(v) = 1 + v/40$$

which corresponds to suppose that, for $v = 40$ m/s, both μ^o and σ^o are half of the corresponding values for $v = 0$. We then assume that $\sigma_i(0) = 0.001$ (this is coherent with a braking maneuver starting at $x_1 = 0$); different values are considered for α in the interval $[\,0.5\,,\,5\,]$ (corresponding to a transient for the braking control systems between 10 s and 1 s); diverse values for the initial speed $v(0)$ and the distance Δ_2 between the braking control units are considered as well. The stopping distance corresponding to the different algorithms are denoted as follows:

- $\mathcal{S}^{\mathrm{Lf}}$ (for the leader–follower approach)
- $\mathcal{S}^{\mathrm{Bd}}$ (for the blind decentralized approach)
- $\mathcal{S}^{\mathrm{Dp}}$ (for the distributed preview approach).

The theoretical limit for the stopping distance, hereafter denoted by $\mathcal{S}^o$, is also computed. This corresponds to the ideal case where, by letting $\mu = \mu^o$ in the equation of v', the dynamics of σ_i is neglected.

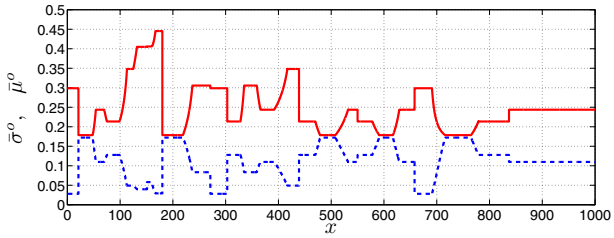

Figure 4. The functions $\bar{\mu}^o(x)$ (continuous red line) and $\bar{\sigma}^o(x)$ (dashed blue line) considered in the simulations.

	$\Delta_2 = 10$m	$\Delta_2 = 25$m	$\Delta_2 = 50$m
$\mathcal{S}^o$	252.77 m	252.08 m	246.16 m
$\mathcal{S}^{\mathrm{Lf}}$	259.59 m	264.25 m	270.26 m
$\mathcal{S}^{\mathrm{Bd}}$	259.79 m	259.72 m	254.43 m
$\mathcal{S}^{\mathrm{Dp}}$	259.20 m	259.40 m	254.11 m

Table 1. Stopping distances for the simulation campaign 1 ($\alpha = 1.5$, $v(0) = 30$).

3.1 Simulation campaign 1

We let $\alpha = 1.5$ s^{-1}, $v(0) = 30$ m/s and simulate the system with the reference generated according to the three approaches (and the ideal one) for values of Δ_2 ranging from 10 m up to 50 m. The resulting stopping distances are in Table 1 and the graphs of the speed are in Figure 5. Let us comment on the simulations:

- The stopping distances resulting from the Bd and the Dp algorithms are close by, but $\mathcal{S}^{\mathrm{Dp}}$ is smaller than $\mathcal{S}^{\mathrm{Bd}}$.
- The performance of the Lf approach are far from those of the Bd and the Dp algorithms, except for $\Delta_2 = 10$ m where the Lf algorithm provides a reasonable (*i.e.,* not too large) anticipation that makes its performance comparable to those of the other approaches. The gap between $\mathcal{S}^{\mathrm{Lf}}$ and the couple $\mathcal{S}^{\mathrm{Bd}}$, $\mathcal{S}^{\mathrm{Dp}}$ is increasing with Δ_2, showing that both the Bd and the Dp approaches are successful when the first and the second coaches are sufficiently far to experience different physical rail conditions.

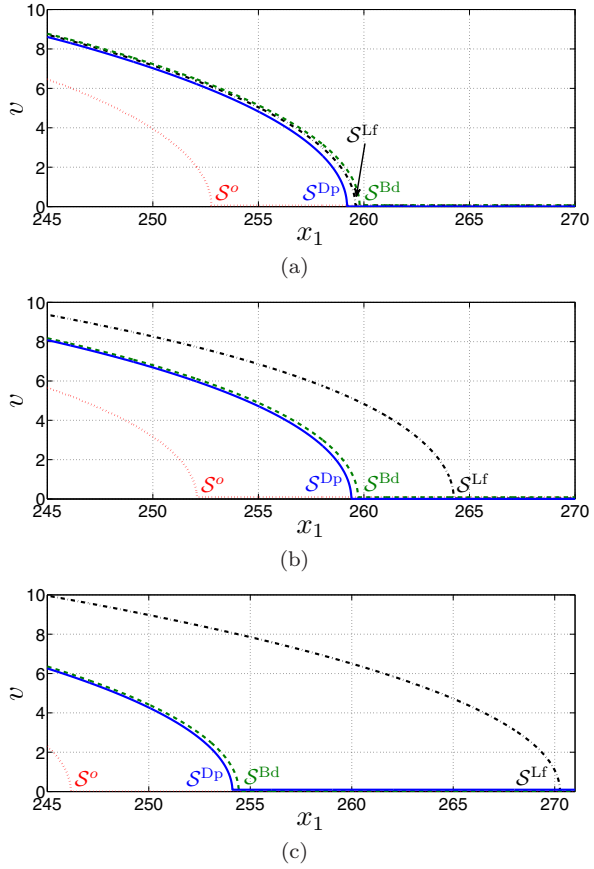

Figure 5. Graphs of the speed in the simulation campaign 1 ($\alpha = 1.5$, $v(0) = 30$): ideal case (dotted red line), Lf approach (dash–dotted black line), Bd approach (dashed green line) and Dp approach (continuous blue line). (a) $\Delta_2 = 10$, (b) $\Delta_2 = 25$, (c) $\Delta_2 = 50$.

In the light of these results, we shall focus on the blind decentralized and the distributed preview algorithms only.

3.2 Simulation campaign 2

We let $v(0) = 50$ m/s, $\Delta_2 = 50$ m and simulate the system according to the Bd and the Dp algorithms (and the ideal one) for values of α ranging from 0.5 up to 5 s^{-1}. The comparison is made according to the following indices:

- $\mathcal{A} = \mathcal{S}^{\mathrm{Bd}} - \mathcal{S}^{\mathrm{Dp}}$ (absolute improvement)
- $\mathcal{A}_{\%} = 100 \cdot \frac{\mathcal{S}^{\mathrm{Bd}} - \mathcal{S}^{\mathrm{Dp}}}{\mathcal{S}^{\mathrm{Bd}}}$ (percentage relative improvement)
- $\mathcal{A}^o_{\%} = 100 \cdot \frac{\mathcal{S}^{\mathrm{Bd}} - \mathcal{S}^{\mathrm{Dp}}}{\mathcal{S}^{\mathrm{Bd}} - \mathcal{S}^o}$ (percentage improvement with respect to the theoretical limit).

We also analyze the tracking error

$$e(x_1) = \begin{bmatrix} e_1(x_1) \\ e_2(x_1) \end{bmatrix} = \begin{bmatrix} \sigma^o\big(x_1, v(x_1)\big) - \sigma_1(x_1) \\ \sigma^o\big(x_1 - \Delta_2, v(x_1)\big) - \sigma_2(x_1) \end{bmatrix},$$

hereafter denoted by e^{Bd} or by e^{Dp} depending on the adopted algorithm to generate the reference signal: we let

$$\begin{cases} n_e^{\mathrm{Bd}} = \frac{1}{\mathcal{S}^{\mathrm{Bd}}} \sqrt{\int_0^{\mathcal{S}^{\mathrm{Bd}}} \|e^{\mathrm{Bd}}(\xi)\|_2^2 d\xi} \\ n_e^{\mathrm{Dp}} = \frac{1}{\mathcal{S}^{\mathrm{Dp}}} \sqrt{\int_0^{\mathcal{S}^{\mathrm{Dp}}} \|e^{\mathrm{Dp}}(\xi)\|_2^2 d\xi} \end{cases}$$

be the normalized $\mathcal{L}^2$–norm of the error signals and consider the percentage relative improvement

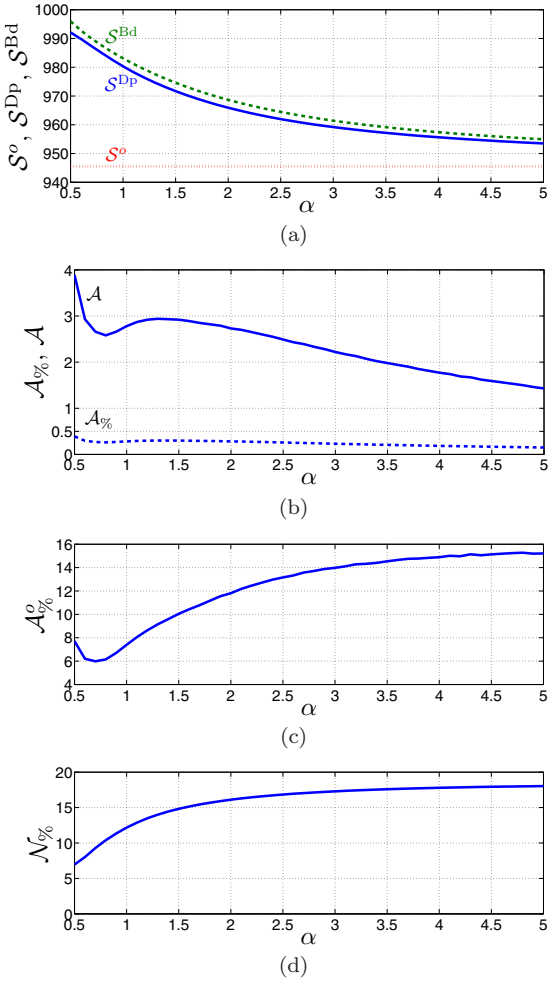

Figure 6. Dependence on α of the indices considered in the simulation campaign 2 ($v(0) = 50$, $\Delta_2 = 50$): (a) stopping distance in the ideal case, with the Bd and with the Dp approach; (b) absolute and percentage relative improvement of the Dp algorithm with respect to the Bd one; (c) percentage improvement with respect to the theoretical limit; (d) percentage relative improvement of the tracking error norm.

$$\mathcal{N}_{\%} = 100 \cdot \frac{n_e^{\mathrm{Bd}} - n_e^{\mathrm{Dp}}}{n_e^{\mathrm{Bd}}}.$$

The behavior of these indices is reported in Figure 6 and it confirms that the Dp approach outperforms the Bd one. More detailed observations are the following:

- The stopping distance decreases as α increases and the absolute improvement borne by the Dp algorithm decreases accordingly (Figure 6.(a–b)). Such decrease is motivated by the corresponding faster dynamics of σ_i that, when $\alpha \to +\infty$, approaches the algebraic relation between Σ_i^o and σ_i yielding $\mathcal{S}^o$. For small values of α, the dynamics of σ_i is so slow that the system mostly operates in transient conditions, thus results are unreliable (see the non-monotonic behaviors of the functions in Figure 6.(b–c)).
- The percentage improvement with respect to the theoretical limit ensured by the Dp algorithm is increasing with α (Figure 6.(c)) and the adoption of a Dp approach allows one to fill up to the 15% of the gap between the performance ensuing from the Bd algorithm and $\mathcal{S}^o$.

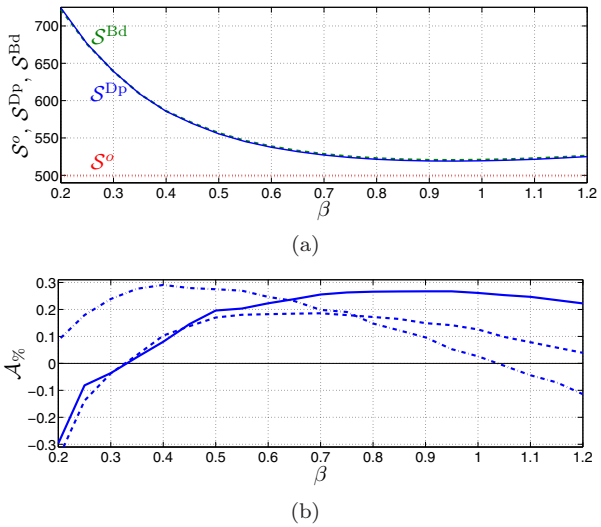

Figure 7. Dependence on β of the indices considered in the simulation campaign 3 $\big(\alpha = 1.5,\ \Delta_2 = 50\big)$: (a) stopping distance in the ideal case, with the Bd and with the Dp approach, when $v(0) = 40$ m/s (for $v(0) = 20$ or 30 m/s the behavior is analogous but shifted below); (b) percentage relative improvement of the Dp algorithm with respect to the Bd one when $v(0) = 20$ m/s (dash–dotted line), $v(0) = 30$ m/s (dashed line) and $v(0) = 40$ m/s (continuous line).

• Also the percentage relative improvement in the tracking error is increasing with α and the enhancement guaranteed by the Dp approach is close to 20% (Figure 6.(d)). Although such a high value of $\mathcal{N}_{\%}$ confirms the soundness of the Dp algorithm, the decrease of the stopping distance is not significant as much. This is mainly due to the fact that the system is controlled so as to operate at $\sigma^o(x, v)$, which is a stationary point of the curve $\mu\big(\theta(x), \cdot, v\big)$: therefore, small displacements of σ_i from the optimal value σ^o result in small differences for the adherence μ. This fact can be interpreted as an intrinsic robustness guaranteed by the control algorithms forcing the system to operate at σ^o.

In practical implementations, the braking control system is often designed so as to track a smaller slip value than the optimal one. Indeed, this policy is more secure in avoiding to drive the system to unstable motions resulting in slip values σ_i making their way towards the highly undesirable condition $\sigma_i = 1$ of locked wheels. In this case, since σ_i is controlled to a non-stationary point of the curve $\mu\big(\theta(x), \cdot, v\big)$, we expect that the Dp approach is capable of guaranteeing more significant improvements. This is analyzed in the next simulation campaign.

3.3 Simulation campaign 3

We let $\alpha = 1.5$ s^{-1}, $\Delta_2 = 50$ m and simulate the system with the reference generated according to the Bd and the Dp algorithms, both scaled by a factor β ranging from 0.2 up to 1.2. In Figure 7, the dependence on β of the stopping distance and of the index $\mathcal{A}_{\%}$ is reported in the three cases where $v(0) = 20$ m/s, $v(0) = 30$ m/s and $v(0) = 40$ m/s.

• While the stopping distance is minimized for $\beta = 1$ (*i.e.*, by tracking the value of σ_i that maximizes the adherence), the percentage relative improvement obtained through the Dp algorithm is maximal for some $\beta < 1$ (thus, providing a larger stopping distance). Such a maximizing β is increasing with the initial speed $v(0)$ and, moreover, the graph of $\mathcal{A}_{\%}(\beta)$ appears to be more and more flat around the maximum as $v(0)$ increases. Consequently, the Dp approach results to be more effective to stop a train running at high speed, where the percentage improvement can be maximized without wasting performance.

• For small or large values of β, the Bd approach may guarantee a shorter stopping distance than the Dp one (see Figure 7.(b)): both cases are not relevant, in practice, since β should not be too small (or else the stopping distance increases too much) or larger than 1 (for security reasons).

We finally mention that the simulations made for a model with three actuated coaches provided analogous results.

4. CONCLUSIONS

A study on the possibility of improving performance in braking maneuvers through the interaction between the control units is presented. A distributed control algorithm based on preview control is proposed and it is shown by simulations to outperform the standard control strategies. Ongoing work is devoted to the extension of the algorithm to more realistic situations where the coaches exchange their *estimates* of the adherence curve. In so doing, other phenomena can be taken into account, such as the cleaning effect. Experimental proofs are *in fieri* as well.

ACKNOWLEDGEMENTS

The work of B. Picasso and D. Caporale was supported by the "Associazione Eugenio e Germana Parizzi" thorugh the "Fondazione Politecnico di Milano". We acknowledge the "Alstom Ferroviaria S.p.a." for useful interactions on the subject of the paper.

REFERENCES

K.B. Ariyur, M. Krstić, "Real-time Optimization by Extremum-Seeking Control", *Wiley*, 2003.
D. Caporale, P. Colaneri, A. Astolfi, "Adaptive nonlinear control of braking in railway vehicles", *52nd IEEE Conference of Decision and Control*, pp. 6892–6897, 2013.
K. Imai, K. Ohishi, T. Sano, S. Makishima, S. Yasukawa, "Real-time Distribution Control of Torque Reference of Commuter Train for Fine Re-adhesion Control", *11th IEEE Int. Workshop on Advanced Motion Control*, pp. 228–233, 2010.
R.H. Middleton, J. Chen, J.S. Freudenberg, "Tracking sensitivity and achievable $\mathcal{H}_\infty$ performance in preview control", *Automatica*, Vol. 40 (8), pp. 1297-1306, 2004.
A.A. Moelja, G. Meinsma, "H_2 control of preview systems", *Automatica*, Vol. 42 (6), pp. 945-952, 2006.
B.J. Olson, S.W. Shaw, G. Stépán, "Nonlinear Dynamics of Vehicle Traction", *Vehicle System Dynamics*, Vol. 40 (6), pp. 377-399, 2003.
O. Polach, "Creep forces in simulations of traction vehicles running on adhesion limit", *Wear*, Vol. 258, pp. 992-1000, 2005.
I. Tyukin, "Adaptation in Dynamical Systems", *Cambridge University Press*, 2011.